Greensphere:
Journal of Environmental Chemistry
ISSN: 2777-0664

Original Article

# Comparative Study of Physical and Chemical Activation of Coal Fly Ash as Potential Adsorbent Based on FTIR and XRD Analyses

**Wayan Gracias[1*], Radho Al Kausar[1], Ermin Riskiani[2]**
[1]Department of Chemistry, Faculty of Mathematics and Natural Sciences, University of Lampung, Jl. Prof. Dr. Soemantri Brodjonegoro 1, Gedong Meneng, Bandar Lampung 35141
[2]Department of Chemistry, Faculty of Mathematics and Natural Sciences, Universitas Gadjah Mada, Bulaksumur, Caturtunggal, Depok, Sleman, Yogyakarta 55281

**Corresponding author*: gracias.wayan@fmipa.unila.ac.id

Received: 29 March 2026 / Accepted: 26 May 2026
Available online: 31 Mei 2026

**Abstrak**

Coal fly ash is a combustion residue that demonstrates potential use an affordable adsorbent. However, the adsorption capacity is still limited if no modification is made, so the activation stage is crucial. The present work investigates the differences between physical and chemical activation on changes in the structure of coal fly ash. Physical activation was carried out through a calcination process at 400 °C within 2 hours, while chemical activation was carried out through a reflux process using a 2 M HCl solution at 50 °C for 6 hours period. The samples were characterized using infrared spectroscopy (FTIR) and X-ray diffraction (XRD) techniques. The obtained results clearly exhibit that physical activation did not cause significant structural changes. In contrast, chemical activation induces partial dealumination in the aluminosilicate framework, which is characterized by a shift in the silanol (Si–O) band from 995 $cm^{-1}$ to 1057 $cm^{-1}$ in the FTIR spectrum, as well as a decrease in mullite intensity and an increase in quartz dominance based on the XRD diffractogram as indicated by the proportion of quartz relative intensity to mullite from 1,000 in CFA to 1,099 and 1,505 respectively in CFAP and CFAC. These changes result in a more silica-rich surface with a higher density of silanol groups, thereby increasing the number of active sites for the adsorption process.

***Keywords:*** *Coal fly ash, Physical activation, Chemical activation, Structural modification, Potential adsorbent*

## 1. Introduction

The sustainability of Indonesia's electricity supply remains heavily reliant on coal, which is the primary fossil fuel. This commodity plays a crucial role, given its role as the primary driver of coal-fired power plant (PLTU) infrastructure. According to official data from the Indonesian Ministry of Energy and Mineral Resources (ESDM), total domestic coal supply is expected to escalate to 790 million tons by 2025, with exports accounting for 65.1% and domestic consumption accounting for 32%, largely absorbed by the electricity sector [1]. Coal-based energy production activities inherently produce considerable amounts of solid waste materials known as fly ash. Coal fly ash (CFA) is a combustion residue composed of fine particles transported along the flue gas stream and subsequently captured using emission control systems. The massive accumulation of this material poses a serious threat to environmental quality if not managed responsibly, as it contains heavy metals that have the potential to leach into the soil and contaminate water bodies through leaching [2].

In recent years, the increasing generation of industrial solid waste has become a major ecological concern worldwide, primarily in developing countries with increasing energy demands [3]. Among various industrial by-products, CFA has become among the most abundantly generated residues due to the continued dependence on coal combustion for electricity generation [4]. The improper disposal of CFA not merely fills up large landfill areas but also contributes to secondary environmental pollution through the release of fine particulates and hazardous inorganic constituents [5]. Therefore, sustainable CFA utilization and valorization strategies are required [6].

On the other hand, CFA has a promising mineralogical composition as an adsorbent candidate because it is rich in inorganic components, which are mainly composed of silica ($SiO_2$), alumina ($Al_2O_3$), and a number of other elements such as iron, calcium, and unburned carbon. The mineralogical structure of CFA is characterized by the presence of crystalline phases including quartz and mullite incorporated into an

amorphous aluminosilicate matrix [7]. Despite its rich aluminosilicate content, the majority of CFA must be modified before being used as an adsorbent to open up its active sites that are still covered by impurities.

To optimize the adsorption performance of CFA, activation requires two main approaches: physical and chemical activation. Physical activation relies on thermal and mechanical treatments to promote higher surface area and enhance the porosity of the material [8], meanwhile, chemical activation utilizes acid or base solutions with the aim of dissolving the impurity phase, opening active sites, and forming functional groups that have higher reactivity towards the adsorbate. [9]. The difference in mechanism between these two approaches directly determines the extent to which the aluminosilicate framework undergoes structural modification.

CFA has been extensively studied as a material for removing heavy metals and dyes from aqueous systems. Several studies have demonstrated the success of chemically treated CFA in adsorbing various contaminants with high efficiency. Hussain [10] reported that acid-base treatment with HCl and NaOH promoted higher surface area in CFA up to three times compared to unmodified CFA, with dye removal efficiency reaching 98%. Nadeem [11] showed that ccid–base activated surface enhanced coal fly ash (SECFA) achieved highly effective crystal violet adsorption with 97.52% efficiency, far exceeding unmodified CFA which only reached 81.52% under the same conditions. Eteba [12] also reported that hydrochloric acid treatment of CFA significantly reduced particle size and increased zeta potential, resulting in dye removal efficiencies of up to 99.7%. In general, these studies confirmed that chemical activation with acidic solutions, especially HCl, resulted in more effective surface modification than untreated CFA.

Despite extensive investigations of CFA in adsorption studies, comparative studies on the effects of physical and chemical activation on changes in the structure and functional groups of the surface, especially on Indonesian CFA, are still limited. [13,14]. Therefore, this study focuses on the comparison of physical activation (CFAP) and chemical activation (CFAC) through the analysis of crystal structure and functional groups using XRD and FTIR [15]. This research does not include adsorption performance testing, but rather focuses on material characterization as a basis for developing CFA-based adsorbents.

## 2. Research Methodology

### 2.1. Equipments and Materials

**Equipments:** This research utilized a number of laboratory equipment, including glassware, an analytical balance (Kern), a hot plate stirrer (ThermoScientific), an oven (InnotechLab), and a muffle furnace (Nabertherm). The material characterization instruments used included an X-ray diffractometer (Xpert PANalytical) and an infrared spectrophotometer (Shimadzu model FT-IR/8201 PC).

**Materials:** The CFA employed in the present study were derived from coal combustion residues at the Paiton Steam Power Plant (PLTU) in East Java. Supporting chemicals included hydrochloric acid (HCl, Merck), a universal indicator (Merck), and distilled water to wash the samples to a neutral pH. All reagents were used as received without additional purification.

### 2.2. Experimental Procedure

#### 2.2.1 Physical Activation of CFA

Physical activation of CFA was carried out through thermal treatment using a muffle furnace. A 25 gram sample of fly ash was heated at 400°C for two hours using an activation furnace. This temperature was chosen because it is within the optimum temperature range for modifying the characteristics of CFA [16,17]. After the heating stage is complete, the material was permitted to cool down to ambient temperature in a desiccator to prevent adsorption of water vapor from the environment. Physically activated samples are designated CFAP (physically activated CFA).

#### 2.2.2 Chemical Activation of CFA

CFA was chemically activated through a reflux process with acid treatment using 2 M HCl solution at an operating temperature of 50 °C for 6 hours with constant stirring. The resulting suspension was then filtered and rinsed with distilled water until neutral pH was achieved [18].

To remove residual moisture, the resulting material was subsequently dried at 105 °C for 6 h and then stored in an airtight condition using a desiccator. The chemically activated sample was designated as CFAC (chemically activated CFA).

#### 2.2.3 Material Characterization

All samples of pre-activated fly ash (CFA), physics activated fly ash (CFAP) and chemically activated fly ash (CFAC) were characterized using infrared spectrophotometer (FTIR) to identify functional groups and structural changes that occurred during activation, as well as X-ray diffraction (XRD) to identify the crystalline phase of the material.

## 3. Results and Discussion

### 3.1. Identification of Functional Groups Using FTIR

To observe structural changes in coal fly ash due to physical and chemical activation treatment, characterization was carried out using FTIR. Overall, all three spectra exhibit similar absorption bands in the wavenumber regions typical for aluminosilicate materials, particularly about ~3400 $cm^{-1}$, ~1057–995 $cm^{-1}$, and ~680–465 $cm^{-1}$ which indicate the presence of hydroxyl groups from water, silanol or aluminum, respectively from the ash fly. The uniformity of this pattern confirms that the basic framework of aluminosilicate is preserved, despite the possibility of local changes in the surface chemical environment due to activation treatment

[19,20]. The FTIR spectra of CFA, CFAP, and CFAC is presented in Figure 1.

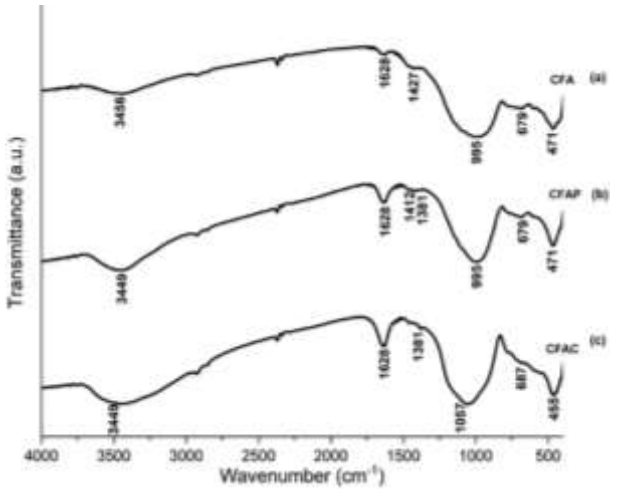


Figure 1: FTIR spectra of (a) CFA; (b) CFAP; (c) CFAC

However, pronounced differences were observed in the peak intensity and peak shifts in CFAC compared to CFA and CFAP. This difference indicates that chemical activation using HCl 2 M produced a more significant structural modification impact than simply providing thermal energy through a furnace. Table 1 shows a summary of absorption interpretations on CFA, CFAP and CFAC.

The absorption band observed in the spectral region around 3400 $cm^{-1}$ corresponds to O–H stretching vibrations, indicating the presence of hydroxyl groups originating from free water molecules. This absorption band generally overlaps with the O–H stretching vibrations of silanol groups present on the surface of the fly ash. [11,13]. After activation, the absorption peak shifted to 3449 $cm^{-1}$ in both CFAP and CFAC. This shift indicates that, in CFAP, furnace heating promoted the release of bound water molecules, resulting in the elongation of hydroxyl bonds and facilitating silanol condensation as well as the rearrangement of hydroxyl groups due to changes in the hydrogen-bonding pattern.

In contrast, in CFAC, treatment with HCl induced protonation of surface hydroxyl groups, making them more prone to interact with water molecules and other surrounding groups. Consequently, the O–H bonds became weaker, and the resulting spectrum broadened due to variations in hydrogen-bonding strength. [18]. The substantial increase in the absorption intensity of hydroxyl groups observed in CFAC indicates the enhancement of active sites in the form of silanol groups following acid activation [14]. The increased density of silanol groups contributes to the enhanced adsorption potential of CFAC, as Si–OH groups function as the primary active sites in surface complexation and ion-exchange mechanisms involving heavy metal cations.

Table 1: Interpretation of the infrared spectrum from CFA, CFAP and CFAC

| Wavenumber ($cm^{-1}$) | | | Interpretation |
|---|---|---|---|
| **CFA** | **CFAP** | **CFAC** | |
| 3456 | 3449 | 3449 | O–H stretching vibrations associated with water molecules and silanol groups (Si–OH) [19,21]. |
| 1628 | 1628 | 1628 | H–O–H bending vibrations [22] |
| 1427 | 1412 | 1381 | Stretching vibrations of carbonate groups or C–O, C–C, and C–H bonds [20,23] |
| 995 | 995 | 1057 | Asymmetric stretching vibrations of Si–O–T bonds (T = Si or Al) [20,24] |
| 679 | 679 | 687 | Symmetric bending vibrations of Si–O–Si or Si–O–Al bonds [24] |
| 471 | 471 | 465 | Symmetric bending vibrations of Si–O–Si bonds [25] |

The alteration of O–H groups is further supported by the appearance of an infrared absorption band at 1628 $cm^{-1}$, which corresponds to the bending vibrations of H–O–H molecules, indicating the presence of adsorbed water molecules on the surface of all CFA samples [22]. The absorption band consistently observed at 1628 $cm^{-1}$ in all samples corresponds to the H–O–H bending vibrations of water molecules trapped on the material surface. In the CFA sample, this band was already present and remained at the same position in CFAP. However, in CFAC, the band became sharper while also exhibiting noticeable broadening. Although no shift in peak position was observed, the change in band profile indicates alterations in the condition and environment of water molecules on the surface. The increased sharpness suggests a more ordered water structure resulting from interactions with newly formed surface sites, whereas the band broadening reflects variations in the molecular environment, likely caused by modifications in the silica network structure during chemical activation [26]. The simultaneous changes observed at 3449 $cm^{-1}$ and 1628 $cm^{-1}$ collectively confirm that chemical activation not only increased the number of silanol groups but also fundamentally altered the interaction characteristics between water molecules and the material surface, ultimately contributing to the enhancement of adsorption active sites in CFAC.

The absorption band in the 1350–1500 $cm^{-1}$ region represents the stretching vibrations of

carbonate groups or organic constituents, including C–O, C–C, –$CH_2$, and –CH bonds [20,23]. In this region, significant differences in the absorption profiles were observed among the three samples. CFA exhibited a peak at 1427 $cm^{-1}$ attributed to the asymmetric stretching vibrations of carbonate groups and organic residues, indicating that the initial surface was still covered by minerals such as calcite [20]. Following physical activation (CFAP), the peak shifted to 1412 $cm^{-1}$ while the absorption intensity remained observable, indicating partial decomposition without complete elimination of impurity phases [13]. In contrast, CFAC exhibited a substantial decrease in absorption intensity accompanied by a peak shift to 1381 $cm^{-1}$, demonstrating that 2 M HCl was considerably more effective through an acid-leaching mechanism. Hydrochloric acid successfully dissolved free carbonates and metal oxides into water-soluble chloride salts, thereby exposing active sites that had previously been blocked. [27].

The most significant structural transformation was observed from the shift of the main peak in the 995–1057 $cm^{-1}$ region, which represents the asymmetric stretching vibrations of Si–O–T bonds (T = Si or Al) within the tetrahedral framework structure of fly ash [20,24]. Both CFA and CFAP exhibited absorption peaks at 995 $cm^{-1}$, whereas CFAC showed a blue shift to 1057 $cm^{-1}$. This shift indicates the occurrence of a dealumination process, in which HCl facilitated the dissolution of aluminum atoms from the aluminosilicate framework, thereby increasing the Si/Al ratio. Since the force constant of siloxane bonds (Si–O–Si) is greater than that of Si–O–Al bonds, the vibrational energy of the framework increased, resulting in a higher wavenumber. This shift also reflects a reduction in Si–O–Al linkages and a relative increase in Si–O–Si bonds, which is consistent with partial dealumination during acid treatment [14]. This finding is further supported by complementary XRD analysis results, as discussed in the following subsection.

### 3.2. Identification of Mineral Phases and Structural Changes Through XRD Analysis

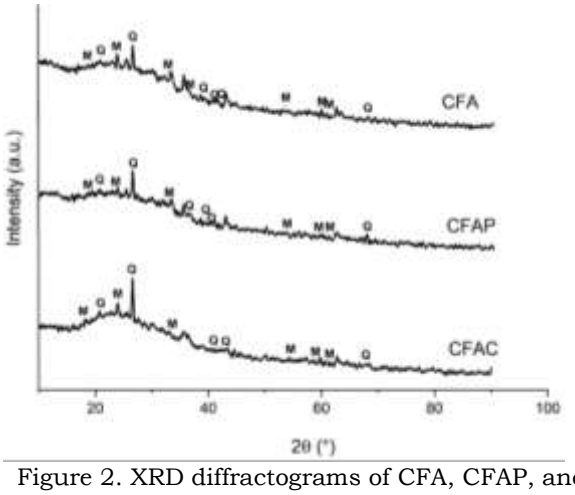


Figure 2. XRD diffractograms of CFA, CFAP, and CFAC (Note: M = Mullite, Q = quartz).

X-ray diffraction characterization was conducted to identify and compare the mineral phases present in CFA, CFAP, and CFAC, as well as to examine the structural changes induced by the activation treatments in a complementary manner to the FTIR analysis findings. The XRD diffractograms of CFA, CFAP, and CFAC are presented in Figure 2, whereas the data on 2θ peak positions, d-spacing values, and phase identification are summarized in Table 2.

Table 2. Diffraction peak positions (2θ), interplanar spacing (d-spacing), and mineral phase identification of CFA, CFAP, and CFAC.

| Sample | 2θ | d-spacing | Mineral Phase |
|---|---|---|---|
| CFA | 18,6004 | 4,7704 | Mullitee |
| | 20,8323 | 4,2641 | Quartz |
| | 23,7047 | 3,7535 | Mullite |
| | 26,5387 | 3,3599 | Quartz |
| | 32,8356 | 2,7254 | Mullite |
| | 36,5917 | 2,4538 | Mullite + Quartz |
| | 38,9612 | 2,3098 | Quartz |
| | 40,1257 | 2,2454 | Mullite |
| | 42,1618 | 2,1416 | Mullite |
| | 53,4220 | 1,7137 | Mullite |
| | 59,6686 | 1,5484 | Mullite |
| | 60,5407 | 1,5281 | Mullite |
| | 68,0216 | 1,3771 | Quartz |
| CFAP | 18,6925 | 4,7471 | Mullite |
| | 20,6571 | 4,2998 | Quartz |
| | 23,5592 | 3,7764 | Mullite |
| | 26,5673 | 3,3552 | Quartz |
| | 32,9794 | 2,7138 | Mullite |
| | 36,2120 | 2,4786 | Quartz + Mullite |
| | 39,3239 | 2,2893 | Quartz |
| | 40,1033 | 2,2466 | Mullite |
| | 53,5785 | 1,7091 | Mullite |
| | 59,6945 | 1,5477 | Mullite |
| | 60,7198 | 1,5278 | Mullite |
| | 67,8427 | 1,3803 | Quartz |
| CFAC | 18,5706 | 4,7780 | Mullite |
| | 20,7289 | 4,2851 | Quartz |
| | 23,9215 | 3,7169 | Mullite |
| | 26,4986 | 3,3637 | Quartz |
| | 32,8727 | 2,7224 | Mullite |
| | 36,4709 | 2,4616 | Mullite + Quartz |
| | 39,3856 | 2,2859 | Quartz |
| | 40,0376 | 2,2502 | Mullite |
| | 42,2761 | 2,1414 | Mullite |
| | 53,7956 | 1,7027 | Mullite |
| | 59,8546 | 1,5439 | Mullite |
| | 60,7591 | 1,5231 | Mullite |
| | 67,8383 | 1,3804 | Quartz |

Based on the XRD analysis results, the crystalline phases of all samples were predominantly composed of Mullite ($3Al_2O_3{\cdot}2SiO_2$, JCPDS No. 15-0776), characterized by an orthorhombic crystal system with lattice parameters of a = 0.7543 nm, b = 0.7693 nm, c =

0.2885 nm, and space group Pbam, as well as Quartz ($SiO_2$, JCPDS No. 46-1045). In addition, a broad hump observed at 2θ = 15–35° indicates the presence of a significant amount of amorphous aluminosilicate matrix. [7,28]. The presence of these two crystalline phases is a typical mineralogical characteristic of Class F fly ash formed from the high-temperature combustion of bituminous coal and is also consistent with the ASTM C618 classification standard [7].

The diffractogram of CFAP was nearly identical to that of CFA, with no indication of new phase formation, confirming that physical activation at 400 °C did not significantly alter the crystalline phase composition. This is attributed to the activation temperature being considerably lower than the degradation temperature of mullite (>1000 °C) and the transformation temperature of quartz to cristobalite (>870 °C) [13]. In contrast, the diffractogram of CFAC exhibited distinct changes, including an increase in the relative intensity of the quartz peak at 2θ ≈ 26.50°, which became sharper and more dominant, accompanied by a decrease in the relative intensity of mullite peaks and alterations in the characteristics of the amorphous hump, indicating modification of the aluminosilicate glass phase due to acid attack. These observations were further supported by semi-quantitative calculations based on the XRD data of all three samples, as presented in Table 3.

Table 3. Comparison of the relative intensities of XRD diffraction peaks in CFA, CFAP, and CFAC.

| Parameter | CFA | CFAP | CFAC |
|---|---|---|---|
| Quartz peak 2θ (°) | 26,56 | 26,56 | 26,58 |
| Mullite peak 2θ (°) | 33,26 | 33,22 | 32,86 |
| Relative Quartz peak intensity with respect to CFA ($I_Q$)(%) | 100,0 | 100,6 | 144,2 |
| Relative Mullite peak intensity with respect to CFA ($I_M$) (%) | 100,0 | 91,5 | 95,8 |
| Quartz/Mullite intensity ratio ($I_Q/I_M$) | 1,000 | 1,099 | 1,505 |
| Relative ratio change with respect to CFA (%) | - | +9,9 | +50,5 |

As presented in Table 3, the relative intensity ratio of quartz to mullite peaks ($I_Q/I_M$) indicates changes in the relative composition of the crystalline phases after treatment. The ratio increased from 1.000 in CFA to 1.099 in CFAP, corresponding to an increase of 9.9%. This relatively minor increase is consistent with previous studies reporting that, in fly ash, significant changes in crystalline phases and enhancement of crystallinity generally become more evident at higher activation temperatures, whereas the presence of mullite and aluminosilicate phases is associated with relatively low material reactivity [29,30].

In contrast, the CFAC sample exhibited an increase in the relative intensity ratio to 1.505, representing a 50.5% increase compared with CFA. This result is consistent with the enhanced sharpness of the quartz peak at 2θ ≈ 26.5° and the relative decrease in mullite peak intensity. These changes indicate that acid treatment modified the amorphous aluminosilicate matrix, causing the quartz phase to become relatively more dominant than the other phases. [31,32].

Furthermore, the increased relative dominance of the quartz phase in CFAC does not indicate the formation of new quartz, but rather results from the partial degradation of Mullite caused by selective dealumination by HCl through the reaction $Al_2O_3 + 6HCl \rightarrow 2AlCl_3 + 3H_2O$. This process produced a silica-rich amorphous surface with a higher density of silanol groups (Si–OH), which function as active adsorption sites through ion-exchange and surface-complexation mechanisms [27,33]. Chemical activation also effectively eliminated secondary impurity phases through carbonate leaching reactions ($CaCO_3 + 2HCl \rightarrow CaCl_2 + H_2O + CO_2$), thereby exposing surface active sites that had previously been blocked, which is consistent with the decrease in the carbonate peak at 1381 $cm^{-1}$ in the FTIR spectrum of CFAC [10].

The shift in the Mullite peak position in CFAC, such as the peak at 2θ = 36.47° (d = 2.4616 Å) compared with 36.59° (d = 2.4538 Å) in CFA, indicates the occurrence of crystalline lattice relaxation due to the extraction of $Al^{3+}$ from the Mullite framework, which was subsequently replaced by silanol groups. This observation is consistent with the blue shift of the Si–O–T peak from 995 $cm^{-1}$ to 1057 $cm^{-1}$ in the infrared spectrum [14]. Overall, the XRD and FTIR analyses indicate that physical activation did not significantly alter the aluminosilicate framework, whereas chemical activation induced selective dealumination, as evidenced by changes in the quartz/mullite peak intensity ratio, shifts in lattice parameters, and an increase in silanol group density. These modifications suggest that CFAC is the most promising adsorbent candidate among the three investigated samples.

## 4. Conclusions

This study demonstrates that chemical activation of coal fly ash produces far more fundamental structural modifications than physical activation. Physical activation at 400 °C did not induce significant changes in the crystalline phases, whereas chemical activation using 2 M HCl promoted selective dealumination of the Mullite framework, as confirmed by the increased dominance of the Quartz peak, the blue shift of the Si–O–T peak from 995 $cm^{-1}$ to 1057 $cm^{-1}$, and the increased density of silanol groups. Semi-quantitative XRD calculations showed that the Quartz/Mullite intensity ratio increased from 1.000 in CFA to 1.505 in CFAC, corresponding to an increase of 50.5%, indicating changes in the crystalline phase distribution after acid treatment. Overall, the characterization results revealed that CFAC possessed a more silica-rich surface with a higher density of silanol groups, highlighting its

potential for further development as an adsorbent material.

**Acknowledgements**
The authors express their appreciation to the Inorganic–Physical Chemistry Laboratory, Department of Chemistry, Faculty of Mathematics and Natural Sciences, Universitas Lampung, for providing the facilities that supported the implementation of this research.

## Bibliography

[1] Kementerian ESDM, Kementerian ESDM RI - Capaian Positif Tahun 2025 (2026). https://www.esdm.go.id/id/media-center/arsip-berita/capaian-positif-tahun-2025-negara-hadir-penuhi-kebutuhan-energi-masyarakat (accessed March 18, 2026).

[2] Y. Chen, Y. Fan, Y. Huang, X. Liao, W. Xu, T. Zhang, A comprehensive review of toxicity of coal fly ash and its leachate in the ecosystem, Ecotoxicol. Environ. Saf. 269 (2024) 115905. https://doi.org/10.1016/J.ECOENV.2023.115905.

[3] N. Ferronato, V. Torretta, Waste Mismanagement in Developing Countries: A Review of Global Issues, International Journal of Environmental Research and Public Health 2019, Vol. 16, Page 1060 16 (2019) 1060. https://doi.org/10.3390/IJERPH16061060.

[4] V.K. Yadav, A. Gacem, N. Choudhary, A. Rai, P. Kumar, K.K. Yadav, M. Abbas, N. Ben Khedher, N.S. Awwad, D. Barik, S. Islam, Status of Coal-Based Thermal Power Plants, Coal Fly Ash Production, Utilization in India and Their Emerging Applications, Minerals 2022, Vol. 12, Page 1503 12 (2022) 1503. https://doi.org/10.3390/MIN12121503.

[5] V.K. Yadav, M.H. Fulekar, Advances in Methods for Recovery of Ferrous, Alumina, and Silica Nanoparticles from Fly Ash Waste, Ceramics 2020, Vol. 3, Pages 384-420 3 (2020) 384–420. https://doi.org/10.3390/CERAMICS3030034.

[6] M. Ragazzi, I. Katsoyiannis, E. Magaril, P. Viotti, H.H. Al-Kayiem, M. Schiavon, G. Ionescu, N. Sliusar, A.Q. Vilakazi, S. Ndlovu, L. Chipise, A. Shemi, The Recycling of Coal Fly Ash: A Review on Sustainable Developments and Economic Considerations, Sustainability 2022, Vol. 14, Page 1958 14 (2022) 1958. https://doi.org/10.3390/SU14041958.

[7] A. Shoppert, I. Loginova, D. Valeev, Kinetics Study of Al Extraction from Desilicated Coal Fly Ash by NaOH at Atmospheric Pressure, Materials 2021, Vol. 14, 14 (2021). https://doi.org/10.3390/MA14247700.

[8] A. Sharma, K. Srivastava, V. Devra, A. Rani, Modification in Properties of Fly Ash through Mechanical and Chemical Activation, Chemical Science International Journal 2 (2012) 177–187. https://doi.org/10.9734/ACSJ/2012/2052.

[9] M.X. Xu, Y.C. Wu, H.W. Ji, X.X. Meng, J.Y. Di, Q. Lu, Preparation of coal fly ash supported high-temperature SCR catalyst by a novel alkali-acid combined activation, Catal. Commun. 180 (2023) 106711. https://doi.org/10.1016/J.CATCOM.2023.106711.

[10] Z. Hussain, N. Chang, J. Sun, S. Xiang, T. Ayaz, H. Zhang, H. Wang, Modification of coal fly ash and its use as low-cost adsorbent for the removal of directive, acid and reactive dyes, J. Hazard. Mater. 422 (2022) 126778. https://doi.org/10.1016/J.JHAZMAT.2021.126778.

[11] H. Nadeem, F. Jamil, M.A. Iqbal, T.W. Nee, M. Kashif, A.H. Ibrahim, S.S. Al-Rawi, S.U. Zia, U.S. Shoukat, R. Kanwal, F. Ahmad, S. Khalid, M.T. Rehman, Comparative study on efficiency of surface enhanced coal fly ash and raw coal fly ash for the removal of hazardous dyes in wastewater: optimization through response surface methodology, RSC Adv. 14 (2024) 22312–22325. https://doi.org/10.1039/D4RA04075A.

[12] A. Eteba, M. Bassyouni, M. Saleh, Modified coal fly ash for textile dye removal from industrial wastewater, Energy & Environment 35 (2024) 1004–1030. https://doi.org/10.1177/0958305X221130536.

[13] A. Kumar, S. Agrawal, N. Dhawan, Processing of Coal Fly Ash for the Extraction of Alumina Values, Journal of Sustainable Metallurgy 6 (2020) 294–306. https://doi.org/10.1007/S40831-020-00275-6/TABLES/3.

[14] Y. Liu, F. Zeng, B. Sun, P. Jia, I.T. Graham, Structural Characterizations of Aluminosilicates in Two Types of Fly Ash Samples from Shanxi Province, North China, Minerals 2019, Vol. 9, 9 (2019). https://doi.org/10.3390/MIN9060358.

[15] M.B. Huda, E. Fachriyah, P.J. Wibawa, Fabrikasi, Karakterisasi, dan Uji Antibakteri Nanopartikel Triterpenoid dari Daun Sambung Nyawa (Gynura procumbens), Greensphere: Journal of Environmental Chemistry 5 (2025) 6–13. https://doi.org/10.14710/GJEC.2025.27478.

[16] E. Misran, O. Bani, S.F. Dina, R. Harahap, N. Wahyuni, Characterization of Coal Fly Ash Based Adsorbent for CO2 Removal, J. Phys. Conf. Ser. 1230 (2019) 012042. https://doi.org/10.1088/1742-6596/1230/1/012042.

[17] O. Ulandari, W. Astuti, S. Sumardi, A. Prasetya, H.T.B.M. Petrus, Synthesis of solid activator for geopolymer product from fly ash and sodium hydroxide, AIP Conf. Proc. 2338 (2021). https://doi.org/10.1063/5.0066649/1027268.

[18] P. Penggunaan Asam Terhadap Pemisahan Logam dari Abu Layang Batubara Sebagai Bahan Dasar Sintesis Zeolit, H. Prihastuti, A. Irawan, T. Kurniawan, Pengaruh Penggunaan Asam Terhadap Pemisahan Logam dari Abu Layang Batubara Sebagai Bahan Dasar Sintesis

Zeolit, Jurnal Kartika Kimia 4 (2021) 13–20. https://doi.org/10.26874/JKK.V4I1.72.

[19] X. Huang, H. Zhao, X. Hu, F. Liu, L. Wang, X. Zhao, P. Gao, P. Ji, Optimization of preparation technology for modified coal fly ash and its adsorption properties for Cd2+, J. Hazard. Mater. 392 (2020) 122461. https://doi.org/10.1016/J.JHAZMAT.2020.122461.

[20] W. Mozgawa, M. Król, J. Dyczek, J. Deja, Investigation of the coal fly ashes using IR spectroscopy, Spectrochim. Acta A Mol. Biomol. Spectrosc. 132 (2014) 889–894. https://doi.org/10.1016/J.SAA.2014.05.052.

[21] J. Yang, H. Sun, T. Peng, L. Zeng, L. Chao, Study on the Overall Reaction Pathways and Structural Transformations during Decomposition of Coal Fly Ash in the Process of Alkali-Calcination, Materials 2021, Vol. 14, 14 (2021) 1–16. https://doi.org/10.3390/MA14051163.

[22] M. Yi, Y. Cheng, C. Wang, Z. Wang, B. Hu, X. He, Effects of composition changes of coal treated with hydrochloric acid on pore structure and fractal characteristics, Fuel 294 (2021) 120506. https://doi.org/10.1016/J.FUEL.2021.120506.

[23] A. Ghofur, Soemarno, A. Hadi, M.D. Putra, Potential fly ash waste as catalytic converter for reduction of HC and CO emissions, Sustainable Environment Research 28 (2018) 357–362. https://doi.org/10.1016/j.serj.2018.07.003.

[24] Z. Yuan, Y. Jia, J. Sun, X. Zhang, Y. Hu, X. Han, Study on the Properties of High Fly Ash Content Alkali-Activated Fly Ash Slag Pastes and Fiber-Reinforced Mortar Under Normal Temperature Curing, Materials 17 (2024). https://doi.org/10.3390/ma17225668.

[25] M. Ritz, Infrared and Raman Spectroscopy of Mullite Ceramics Synthesized from Fly Ash and Kaolin, Minerals 13 (2023) 864. https://doi.org/10.3390/MIN13070864/S1.

[26] G. Cheng, M. Zhang, Y. Zhang, B. Lin, H. Zhan, H. Zhang, A novel renewable collector from waste fried oil and its application in coal combustion residuals decarbonization, Fuel 323 (2022) 124388. https://doi.org/10.1016/J.FUEL.2022.124388.

[27] Z. Lv, X. Pan, X. Geng, H. Yu, Synergistic removal of calcium and iron impurities from calcium-rich and high-alumina fly ash by acid leaching control, J. Environ. Chem. Eng. 10 (2022) 107268. https://doi.org/10.1016/J.JECE.2022.107268.

[28] K.M. Abas, N.A. Fathy, Sodalite zeolitic materials produced from coal fly ash for removal of congo red dye from aqueous solutions, International Journal of Environmental Science and Technology 21 (2024) 5165–5184. https://doi.org/10.1007/S13762-023-05347-0/FIGURES/15.

[29] S. Katara, S. Kabra, A. Sharma, R. Hada, A. Rani, Surface Modification of Fly Ash by Thermal Activation: A DR/FTIR Study, Int. Res. J. Pure Appl. Chem. 3 (2013) 299–307. https://doi.org/10.9734/IRJPAC/2013/4287.

[30] S. Li, P. Bo, L. Kang, H. Guo, W. Gao, S. Qin, Activation Pretreatment and Leaching Process of High-Alumina Coal Fly Ash to Extract Lithium and Aluminum, Metals 2020, Vol. 10, Page 893 10 (2020) 893. https://doi.org/10.3390/MET10070893.

[31] V. Gilja, Z. Katancic, L.K. Krehula, V. Mandic, Z. Hrnjak-Murgic, Eflciency of TiO2 catalyst supported by modified waste fly ash during photodegradation of RR45 dye, IEEE Journal of Selected Topics in Quantum Electronics 26 (2019) 292–300. https://doi.org/10.1515/SECM-2019-0017/ASSET/GRAPHIC/J_SECM-2019-0017_FIG_007.JPG.

[32] A. Eteba, M. Bassyouni, M. Saleh, Utilization of chemically modified coal fly ash as cost-effective adsorbent for removal of hazardous organic wastes, International Journal of Environmental Science and Technology 20 (2023) 7589–7602. https://doi.org/10.1007/S13762-022-04457-5/TABLES/5.

[33] J.M. Gao, Z. Yan, S. Ma, Y. Guo, Novel process for high value utilization of high-alumina fly ash: valuable metals recovery and mesoporous silica in situ preparation, RSC Adv. 14 (2024) 1782–1793. https://doi.org/10.1039/D3RA06921D.